



Phosphorus adsorption by sediment considering mineral composition and environmental factors

Xiaocui Li¹ · Lei Huang¹ · Hongwei Fang¹ · Minghong Chen² · Zhenghui Cui³ · Zhiyu Sun⁴ · Danny Reible⁵

Received: 29 January 2020 / Accepted: 22 December 2020 / Published online: 4 January 2021
© The Author(s), under exclusive licence to Springer-Verlag GmbH, DE part of Springer Nature 2021

Abstract

Sediment, composed of a complex assemblage of minerals, controls the fate and behaviour of P in aqueous environments and affects trophic status. In this study, P adsorption was studied on minerals including quartz, hematite, potassium feldspar, montmorillonite, kaolin, and calcite (i.e., the main components of sediment) and sediment from the Guanting Reservoir. A general formula for P adsorption was proposed that considers mineral composition through the component additivity method, also incorporating the effects of environmental factors, including the aqueous P concentration (C_e), pH, sediment concentration (S), and ionic strength (IS). The P adsorption capacity gradually decreased with increasing particle size, and the contributions from kaolin and montmorillonite to P adsorption were significant despite representing only a small fraction of sediment (with a maximum amount of P adsorption of 0.92 and 0.36 mg/g, respectively). The content of quartz accounted for approximately 40–60% of sediment; however, its P adsorption capacity was only 0.13 mg/g. These minerals exhibited different adsorption characteristics due to their different surface morphologies and lattice structures. Multivariable regression analysis was used to show that the amount of P adsorption was strongly correlated with C_e , followed by S , IS, and pH.

Keywords Sediment · Adsorption capacity · Phosphorus · Component additivity method · Environmental factors

Introduction

Water pollution in many rivers and reservoirs has attracted serious attention due to an excess supply of nutrients and other

contaminants (Xu et al. 2010). Phosphorus (P) is a key nutrient for phytoplankton growth and production but is also the major controlling factor for eutrophication (Huang et al. 2015a). Sediment has a strong affinity for soluble active P

Xiaocui Li and Lei Huang contributed equally to this work.

Highlights

- The adsorption properties of minerals are affected by surface morphology and lattice structures.
 - Clay minerals greatly contribute to the P adsorption by sediment despite the low contents.
 - The amount of P adsorption is strongly correlated with aqueous P concentration.
 - A general formula of P adsorption is proposed considering mineral composition and environmental factors.
-

Responsible Editor: Christian Gagnon

✉ Lei Huang
huanglei2017@tsinghua.edu.cn

✉ Hongwei Fang
fanghw@tsinghua.edu.cn

¹ State Key Laboratory of Hydro-science and Engineering, Department of Hydraulic Engineering, Tsinghua University, Beijing 100084, China

² College of Water Resources and Civil Engineering, China Agricultural University, Beijing 100083, China

³ China Renewable Energy Engineering Institute, Beijing 100120, China

⁴ China Three Gorges Corporation, Beijing 100038, China

⁵ Department of Civil & Environmental Engineering, Texas Tech University, Lubbock, TX 79409-1023, USA

due to its high specific surface area and adsorption (Chen and Fang 2013; Huang et al. 2015b; Lopez et al. 1996; Zhao et al. 2015), and P adsorption by sediment is an important process for regulating the mobilization and dynamics of P (An and Li 2009; Zhou et al. 2005). For example, adsorbed P may accumulate on the bed surface with sediment deposition, and accumulated P may be released back into the overlying water when physiochemical factors shift or due to changes in hydrodynamic conditions (e.g., sediment erosion) (Jarvie et al. 2005; Jin et al. 2005; Zhang et al. 2007). Therefore, it is essential to understand P adsorption by sediment to understand and manage water quality.

Adsorption is the accumulation of substances at the interfaces, e.g., solid/liquid interfaces, which is an extremely complex phenomenon and is affected by both intrinsic and extrinsic factors (Sundareshwar and Morris 1999). Intrinsic factors mainly refer to the characteristics of the sediment itself, such as particle size (Meng et al. 2014; Selig 2003; Stone and Mudroch 1989), surface micromorphology (Fang et al. 2013), mineral composition (Wang et al. 2009), and organic matter content (Liu and Lee 2007). Extrinsic factors mainly refer to a variety of environmental factors, such as the aqueous P concentration (C_e), pH (Huang et al. 2016; Palleyi et al. 2015), sediment concentration (S) (Huang et al. 2017), ionic strength (IS) (Aldegs et al. 2008; Kafkafi et al. 1988), and temperature (Huang et al. 2011). Over the past several decades, scientists have investigated various extrinsic and intrinsic factors in regard to P adsorption, and our understanding of P adsorption has improved.

Sediment is a complex assemblage of various minerals, such as quartz, feldspar, oxides, and clay minerals, and the mineral composition largely depends on the climatic environment (Dickens et al. 2006; Wakeham et al. 2009). Yang et al. (2002) studied the fine sediment in the Yangtze River Estuary and Yellow River Estuary and found that the sediment consisted of approximately 40% quartz, 30% feldspar, and 5% calcite, with the remaining material primarily containing clay minerals such as kaolin, montmorillonite, and illite. Tang et al. (2000) summarized the relative composition of clay minerals in sediment from major rivers of China, as listed in Table A1. The mineral composition significantly affects P adsorption due to the different surface morphologies and lattice structures. For example, Wang et al. (2005) studied P adsorption on sediment from the Yangtze River and observed that the maximum P adsorption amount (i.e., the P adsorption capacity) increased in proportion to aluminium (Al), iron (Fe), and calcium (Ca). Similar results were also found by other researchers (Furumai et al. 1989; Tang et al. 2014). Moreover, Cui et al. (2017) and Fang et al. (2017) found that surface heterogeneity due to mineral composition plays an important role in P adsorption by sediment. Nevertheless, there exists no method to quantitatively predict P adsorption by sediment that is composed of various minerals.

A number of adsorption isotherms have been widely applied to quantitatively describe adsorption at the equilibrium state (Mortula et al. 2007; Ushiki et al. 2014; Wang et al. 2017). For example, the Langmuir adsorption isotherm was developed to describe uniform monolayer adsorption (Langmuir 1916, 1917, 1918), and the Freundlich isotherm has been applied to multilayer heterogeneous adsorption (Foo and Hameed 2010; Malek and Farooq 1996). These empirical isotherms, however, do not indicate how mineral composition affects adsorption. In this study, the effects of mineral composition on P adsorption are quantified based on adsorption experiments, while simultaneously considering environmental factors (including C_e , pH, S , and IS), and then, a general formula of P adsorption by sediment is proposed, which can aid in the understanding of the fate and transport of P in aqueous systems.

Materials and methods

Materials and analytical methods

Both pure mineral and sediment samples were used for the P adsorption experiments. The pure minerals samples were purchased from the National Center of Reference Material (NCRM) of China, including quartz, hematite, potassium feldspar, montmorillonite, kaolin, and calcite, which are the main components of sediment. Sediment was collected from the Guanting Reservoir, China, using a core sampling device and stored in precleared polyethylene bags at 4 °C. Guanting Reservoir was once one of the main water sources in Beijing but was withdrawn from the urban drinking-water system in 1997 because of poor water quality (He et al. 2011). To accurately and quantitatively describe the influence of sediment mineral composition on P adsorption, sediment samples were repeatedly washed with hydrogen peroxide, concentrated hydrochloric acid, and deionized water to minimize the interference from surface pollutants (e.g., humic acid, organic matter, and ions): (1) mix sediment samples and deionized water in a conical flask and then add hydrogen peroxide; wash repeatedly with deionized water when the reaction is sufficient (no more bubbles and heat release) and then pour out the supernatant; and (2) add concentrated hydrochloric acid and deionized water into the conical flask and stir thoroughly and then wash with deionized water until the filtrate was neutral. More details can be found in Fang et al. (2008, 2014). Hei et al. (2017) suggested that this cleaning method can remove most surface pollutants, and the main composition and structure of sediment do not change greatly. Finally, the cleaned sediment samples were dried in an oven at 105 °C for 24 h.

The grain size of the mineral and sediment samples was measured using a laser scattering particle size distribution analyser (HORIBA LA-920, Japan). The specific surface area

(SSA) was determined by nitrogen (N_2) adsorption/desorption isotherms using the Brunauer-Emmett-Teller (BET) method (ASAP2020 M, Micromeritics, USA). Scanning electron microscopy (SEM, JEOLJSM-6310F) was employed to analyse the surface morphology and microstructure, which was conducted at the School of Materials Science and Engineering, Tsinghua University, and an average morphology descriptor F_{2a} (supplementary information) was then derived that can be used to predict adsorption onto pure minerals (Cui et al. 2017). The surface-active site densities (N_s) of minerals were estimated with crystallographic characterization from the literature (Venema et al. 1998; White and Zelazny 1988; Wieland and Stumm 1992) and then refined by optimization to fit the adsorption data with MINTEQA2 software, following the methods provided by Hayes et al. (1991). X-ray diffraction analysis (Dmax-RB 12 kW, Rigaku, Japan) was performed to obtain the mineral composition of the sediment.

Adsorption experiment

For each mineral sample, 0.5 g samples were added to 30 mL of P solution (anhydrous KH_2PO_4) with initial P concentrations of 0.0, 0.8, 1.0, 2.0, 3.0, 5.0, 8.0, 10.0, 15.0, and 20 mg/L. Batch experiments were performed in an incubator shaker continuously shaking at 20 ± 2 °C with an oscillation rate of 190 rpm for 24 h. Preliminary kinetic experiments have shown that equilibrium adsorption can be achieved within 24 h. After adsorption, the tubes were centrifuged, and the supernatant solutions were extracted and filtered through a 0.45 μm cellulose ester filter membrane for the measurement of P concentration using the ammonium molybdate spectrophotometric method (Ministry of Environment Protection of China (MEP) 2001). Then, the adsorbed P was calculated from the difference between the concentrations before and after adsorption. All adsorption experiments were performed in duplicate.

For the cleaned sediment samples from Guanting Reservoir, 0.15, 0.30, and 0.45 g samples were added to 30 mL of P solution (anhydrous KH_2PO_4) with initial P concentrations of 1, 2, 3, 4, 5, 8, and 10 mg/L. The samples were then processed in the same manner as the pure mineral samples. P adsorption results from sediment from natural rivers, lakes, and reservoirs were also collected from the literature for analysis and comparison.

Formula derivation

Similar to the Langmuir adsorption isotherm, the amount of P adsorption by minerals and sediment at equilibrium, q_e , can be expressed as a product of the maximum adsorption amount (adsorption capacity), Q_{max} , and the function of environmental factors, F , i.e.,

$$q_e = Q_{max} \cdot F(\text{Environmental factors}) \tag{1}$$

The maximum adsorption amount, Q_{max} , is mainly determined by intrinsic particle factors, particularly particle specific surface area (SSA), and mineral composition. The finer the particle size is, the larger the SSA and the greater the adsorption capacity (Wang et al. 2006). Moreover, the surface structures of various minerals are different, providing different surface morphologies and active site densities, thus exerting different effects on adsorption (Gao et al. 2014; Prarat et al. 2011). Fang et al. (2017) introduced a comprehensive factor, I , to represent the basic properties of mineral particles, i.e.

$$I(D_{50}, N_s, F_{2a}) = \frac{N_s}{\rho} \left(\frac{2}{D_{50}} \right)^{1.85 F_{2a} + 0.60} \tag{2}$$

where D_{50} is the median particle size, N_s is the surface-active site density determined from crystallographic characterization, F_{2a} is an average morphology descriptor calculated from the SEM images that indicates the degree of heterogeneity or roughness of particle surfaces (Fang et al. 2017), the detailed formula for F_{2a} is in the supplementary information, and ρ is the particle density. I reflects the concentration of surface-active sites, and the maximum adsorption amount is assumed to be linearly related to I , i.e.,

$$Q_{max} = f(I) = a \cdot I + b \tag{3}$$

where a and b are unknown parameters to be determined. First, pure mineral particles were observed using SEM to characterize the local micromorphology and to derive the average morphology descriptor F_{2a} . Then, the comprehensive factor, I , was calculated incorporating the values of the particle size, D_{50} , and surface-active site density, N_s (see Eq. (2)). Subsequently, a relation between Q_{max} and I can be established based on the results of the adsorption experiment, i.e., Eq. (3).

Moreover, sediment is an assemblage of various minerals; thus, the maximum adsorption amount of sediment, Q_{max}^s , might be further calculated using the component additivity method from pure minerals (Davis et al. 1998), i.e.,

$$Q_{max}^s = \sum(p_i \cdot Q_{max}^i) \tag{4}$$

where p_i and Q_{max}^i represent the mass percentage and maximum adsorption amount of the i th mineral, respectively. For example, Schaller et al. (2008) studied the adsorption of copper ions (Cu^{2+}) on pure ferric oxide, pure kaolin, and their mixtures and found that component additivity was in good agreement with the predicted Cu^{2+} adsorption.

In addition, the effects of extrinsic factors can be regarded as individual functions of the environmental factors. Here, the major factors include the aqueous P concentration, C_e , pH, ionic strength, IS , and sediment concentration, S , i.e.,

$$F(\text{Environmental factors}) = f(C_e) \cdot f(pH) \cdot f(IS) \cdot f(S) \tag{5}$$

The amount of P adsorption by sediment is affected by these factors simultaneously (Ku et al. 1978); therefore, both individual factor and multivariable regression analyses were conducted, and expressions for $f(C_e)$, $f(\text{pH})$, $f(\text{IS})$, and $f(S)$ were mainly derived from data in the literature.

Finally, the amount of P adsorption by sediment at equilibrium can be expressed as

$$q_e = Q_{\max}^s \cdot f(C_e) \cdot f(\text{pH}) \cdot f(\text{IS}) \cdot f(S) = \sum (p_i \cdot Q_{\max}^s) \cdot f(C_e) \cdot f(\text{pH}) \cdot f(\text{IS}) \cdot f(S) \quad (6)$$

Results and discussion

Physicochemical properties of sediment and pure minerals

The physical and chemical properties of these pure minerals are listed in Table 1. The median particle size D_{50} of the pure minerals is in the range of 7.65–15.12 μm , with an average value of 11.08 μm . Figure 1(a–f) shows the SEM images of quartz, hematite, potassium feldspar, montmorillonite, kaolin, and calcite, indicating extremely complex surface morphology that significantly affects P adsorption. The surface morphology of montmorillonite and kaolin (i.e., clay minerals) is more complex, leading to a greater SSA, i.e., 14.07 and 35.74 m^2/g , respectively, while the SSAs of the other minerals are only 1.64–4.11 m^2/g . According to their three-dimensional (3D) surface morphology, an average morphology descriptor, F_{2a} , was derived through Taylor expansion, which can reflect the degree of surface heterogeneity of particles. Accordingly, montmorillonite and kaolin exhibit greater F_{2a} values of 0.168 and 0.184, respectively, followed by hematite, potassium feldspar, quartz, and calcite. Here, a total of 100 particles were analysed for each mineral, with additional sediment particles exerting only little effect on the results. Moreover, hematite has a relatively large N_s of 5.35 site/nm^2 and a large particle density of 5.10 g/cm^3 .

Moreover, D_{50} of the cleaned sediment samples is approximately 9.77 μm with SSA of 26.7 m^2/g . X-ray diffraction analysis shows that the cleaned sediment is composed of

40% quartz, 20% feldspar, and 10% calcite, and the remaining sediment is composed of clay minerals and a small amount of amphibole. The SEM images of natural sediment (i.e., before sediment cleaning) and cleaned sediment are shown in Fig. 1g, h, respectively. It is evident that the surface morphology of natural sediment is more complex, and the particle surface is basically wrapped by a layer of film, flocculent or clastic material, forming many dense pore structures. Most of the adherents on the particle surface have been washed away in the cleaned sediment, as shown in Fig. 1h, and the shape of the original sediment particles is present. Although the morphological characteristics of the cleaned sediment are very different from those of the natural sediment, the main composition and structure of the sediment do not change greatly after repeated washing. There are a few fine particles attached to the cleaned sediment surface, which may be organic matter that has not been removed or fine particles reattached during drying and storage.

P adsorption by pure minerals

To elucidate the effects of mineral composition on P adsorption by sediment, it is necessary to first study the characteristics of P adsorption by pure minerals. The measured maximum P adsorption amounts of these minerals under the experimental conditions described in “Adsorption experiment” are also listed in Table 1, with the average value ranging from 0.11 to 0.92 mg/g . The P adsorption amount by different minerals varies greatly, mainly due to the different surface morphologies and lattice structures. Most of the clay minerals (e.g., montmorillonite and kaolin) are composed of layers of silicon-oxygen tetrahedra and aluminium-oxygen octahedra, generally leading to large SSA, strong ion-exchange capacities, and significant P adsorption (Uddin 2017). Thus, although quartz, hematite, montmorillonite, and kaolin have similar particle sizes (approximately 10 μm), their adsorption amounts are quite different, i.e., 0.13, 0.11, 0.36, and 0.92 mg/g , respectively.

Based on the basic characteristics of each mineral (i.e., D_{50} , F_{2a} , N_s , and ρ in Table 1), the comprehensive factor, I , can be

Table 1 Physicochemical properties of minerals and the measured maximum adsorption amount

Minerals	D_{50} (μm)	Specific surface area SSA (m^2/g)	F_{2a}	Surface active site density N_s (site/nm^2)	Particle density ρ (g/cm^3)	Q_{\max} (mg/g)
Quartz	11.37	1.64	0.114	4.80	2.65	0.13
Hematite	11.40	2.86	0.142	5.35	5.10	0.11
Potassium feldspar	7.65	4.11	0.131	4.25	2.65	0.26
Montmorillonite	9.91	14.07	0.168	2.06	2.60	0.36
Kaolin	11.01	35.74	0.184	3.63	2.57	0.92
Calcite	15.12	3.91	0.106	5.00	2.70	0.31

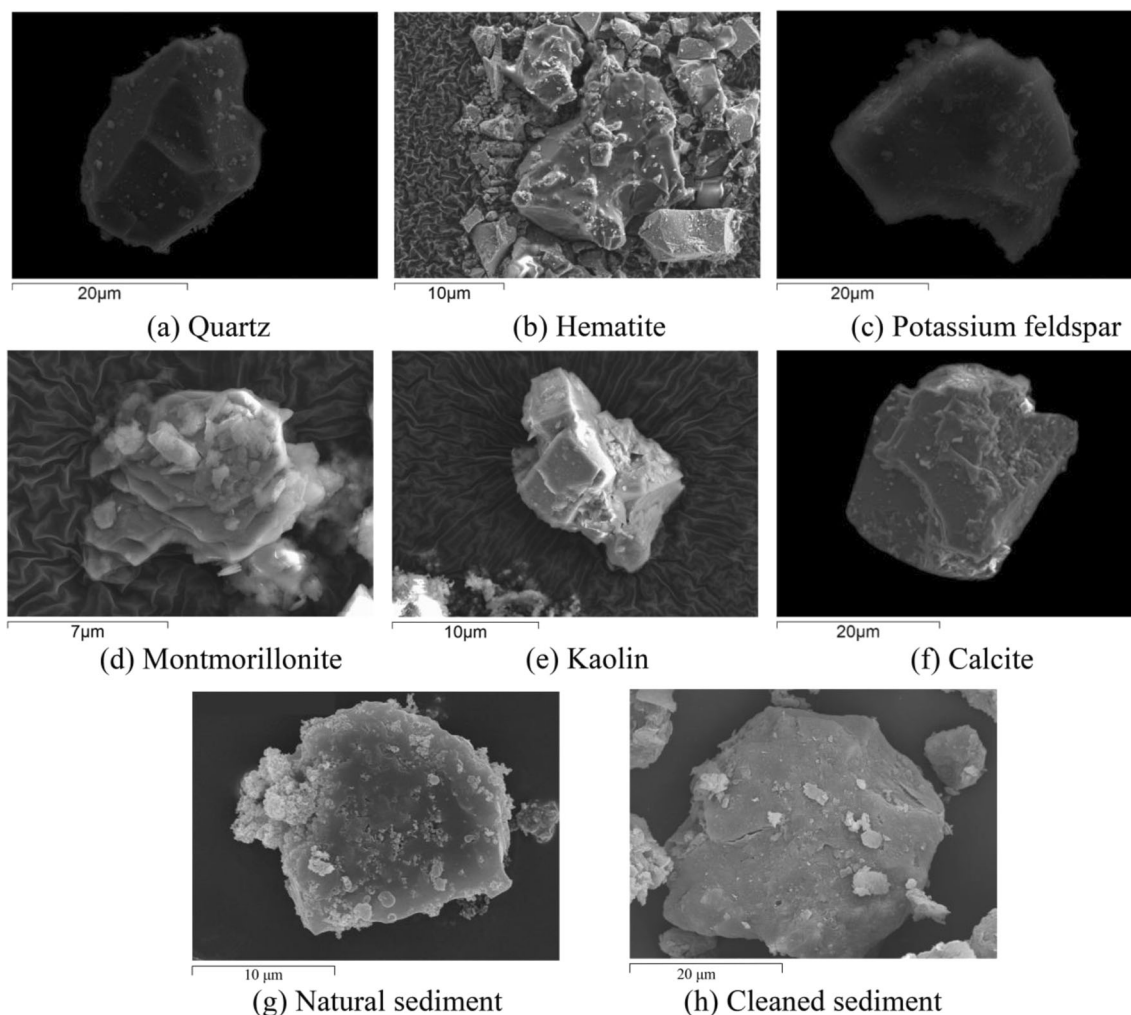
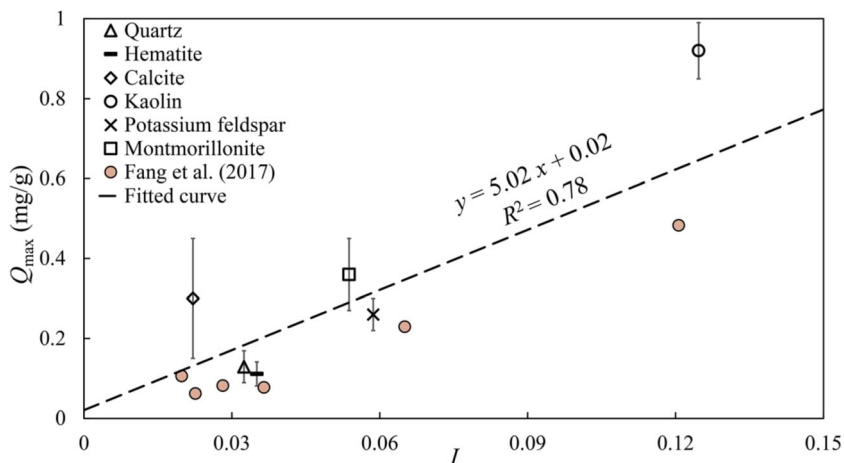


Fig. 1 SEM images of pure minerals and sediment. **a** Quartz. **b** Hematite. **c** Potassium feldspar. **d** Montmorillonite. **e** Kaolin. **f** Calcite. **g** Natural sediment. **h** Cleaned sediment

calculated according to Eq. (2). Then, the relation between Q_{max} and I for minerals is established incorporating the measured maximum adsorption amount, as shown in Fig. 2, with the different minerals represented by different symbols.

Moreover, the experimental data of Fang et al. (2017) are also shown using solid dots. The dotted line represents the best fitting line ($R^2 = 0.78$), and the fitting parameters are $a = 5.02$ and $b = 0.02$, i.e.,

Fig. 2 Relationship between the adsorption capacity Q_{max} and comprehensive factor I



$$Q_{\max} = f(D) = 5.02D + 0.02 \quad (7)$$

In addition, particle size also has a significant effect on P adsorption (Shi et al. 2018), as finer particles generally have a greater SSA and more potential surface-active sites, leading to a larger adsorption capacity. For example, calcite with a median size of 36.89 μm was also used in the P adsorption experiment, and the observed maximum adsorption amount was only 0.12 mg/g (the result is not listed in Table 1), which is much smaller than the value of 0.31 mg/g for calcite with a size of 15.12 μm . The variations in P adsorption capacity with particle size for pure minerals are shown by dotted lines in Fig. 3, as calculated from Eqs. (2) and (7). Apparently, the maximum P adsorption amount decreases with increasing particle size, and kaolin exhibits the greatest Q_{\max} among these minerals at the same particle size.

P adsorption by sediment

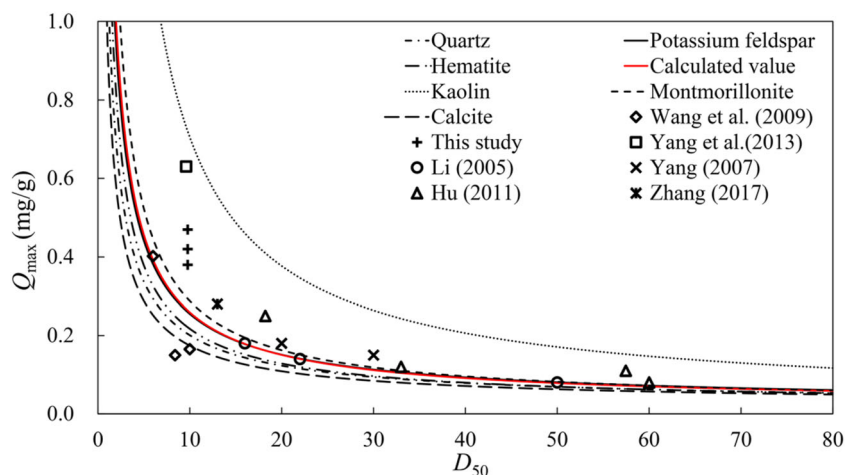
The red line in Fig. 3 shows the variation of the maximum P adsorption amount with particle size for sediment, which is derived from the pure minerals using the component additivity method, i.e., Eq. (4). Thus, given the particle size and mineral composition, the P adsorption capacity of sediment can be directly obtained. Here, the mineral composition of sediment from Guanting Reservoir was simply adopted, i.e., 40% quartz, 20% feldspar, and 10% calcite, with the remaining minerals consisting of clay minerals and amphibole (Huang et al. 2015a; Zhao et al. 2011). As shown in Fig. 3, the P adsorption by sediment exhibits the same trend with increasing particle size as that of minerals, and the calculated P adsorption capacity of sediment is within the range of that of pure minerals. It is worth noting that although the contents of clay minerals (kaolin and montmorillonite) are small in sediment, their P adsorption capacities are much larger than those

of other minerals at similar particle sizes, which may greatly contribute to the P adsorption by sediment (Li et al. 2019).

The experimental results of P adsorption by cleaned sediment from this study and natural sediment from the literature are also shown in Fig. 3 using different symbols, and more information on these data is provided in Table A2. Here, the results with similar experimental conditions as those in this study, such as a pH of 6–8 and a sediment concentration of 1–2 g/L, are chosen (except Wang et al. 2009). Overall, the experimental results are close to the calculated values for sediment (i.e., the red line in Fig. 3), especially for the relatively coarse sediment, indicating that Eq. (4) can reasonably predict the maximum P adsorption amount of sediment. The differences between the calculated and measured P adsorption capacities may be primarily due to the lack of mineral compositional data, which are not provided in the literature; therefore, the mineral composition of sediment from the Guanting Reservoir was simply adopted, as previously described.

The mineral composition of sediment is also related to the particle size. For example, previous studies have shown that sediment in the lower reaches of rivers or estuaries (with a high level of fine-grained particles) is mainly composed of clay minerals and oxides (Edzwald et al. 1976; Gérard 2016; Shao et al. 2014). Li et al. (2012) studied the correlation between the particle size and mineral composition of sediment from the Three Gorges Reservoir, in which more quartz and feldspar were observed in coarse sediment, while more clay minerals were observed in relatively fine-grained sediment. Thus, there should be a sharper increase in the P adsorption capacity with decreasing particle size than that shown by the red line in Fig. 3, especially when $D < 10 \mu\text{m}$, which partially explains the differences between the calculated and measured P adsorption capacities. Furthermore, the surface pollutants (e.g., humic acid, organic matter, and ions) of natural sediment may also contribute to these differences, and it is observed that the measured P adsorption capacity was generally greater than the calculated values.

Fig. 3 Variation in the maximum P adsorption amount with particle size (note: the dotted and solid lines represent the calculated results for minerals and sediment, respectively, using Eqs. (2), (4), and (7); the symbols represent the experimental results from the literature)



Moreover, the experimental results of natural sediment are generally within the range of pure minerals, as shown in Fig. 3, also indicating that the mineral composition plays a key role in the adsorption properties of natural sediment and that the component additivity method can be applied in this study.

Effects of environmental factors on P adsorption by sediment

The amount of P adsorption by sediment at equilibrium, q_e , is affected by environmental factors, making it difficult to achieve the adsorption capacity, Q_{max}^s . According to Eq. (6), the function of the environmental factors can be expressed as

$$F(\text{Environmental factors}) = \frac{f(C_e) \cdot f(\text{pH}) \cdot f(IS) \cdot f(S)}{\sum(p_i \cdot Q_{max}^s)} = \frac{q_e}{Q_{max}^s} \tag{8}$$

Therefore, the detailed expressions of $f(C_e)$, $f(\text{pH})$, $f(IS)$, and $f(S)$ can be derived from the relationships between q_e/Q_{max}^s and each environmental factor through individual factor or multivariable regression analyses.

The effect of aqueous P concentration was assumed to be given by the Langmuir adsorption isotherm, $f(C_e) \propto k_1 \frac{C_e}{1+k_1 C_e}$, where k_1 is a constant related to the affinity of sediment to phosphate ions ($k_1 > 0$). The amount of P adsorption varies with the pH due to the electrostatic interactions between the charged sediment surface and phosphate ions, i.e., the positive charge on sediment surfaces increases gradually with a decrease in pH, and the amount of P adsorption increases accordingly.

The influence of pH on P adsorption is assumed to be a power function, i.e., $f(\text{pH}) \propto \text{pH}^{k_2}$ (Huang et al. 2016; Pagnanelli et al. 2003). Although the total amount of P adsorption increases with increasing S , the amount of P adsorption per gram of sediment decreases due to the more significant effects of competitive adsorption under a higher S (Huang et al. 2017). An exponential relation between the amount of P adsorption and S can be adopted, i.e., $f(S) \propto e^{k_3 S}$. There are relatively few studies about the effect of IS on P adsorption by sediment, and some inconsistent results exist. For example, Li et al. (2005) showed that a higher IS was generally favourable for P adsorption by sediment, but anions such as SO_4^{2-} , F^- , $\text{B}(\text{OH})_4^-$, and OH^- may compete with phosphate ions for the surface adsorption sites and reduce the amount of P adsorption. Wang et al. (2005) concluded that the amount of P adsorption decreased with increasing IS . Here, it is assumed that the effect of IS on P adsorption can be expressed as $f(IS) \propto e^{k_4 \cdot IS}$. The individual factor analysis of the relation between q_e/Q_{max}^s and C_e , pH, S , and IS is plotted in Fig. 4, where the data from different researchers are represented by different symbols or colours (for more information on these data, see Table A2).

In Fig. 4, the dashed lines represent the fitting functions, and the values of k_1 , k_2 , k_3 , and k_4 are fitted as 0.65, -0.923 , -0.022 , and -25 , respectively. It is worth noting that the amount of P adsorption by sediment decreased significantly when the pH was too low (e.g., less than 2–3) due to the dissolution of Fe and Al compounds in the sediment (see the red-dashed line in Fig. 4(b)); therefore, the function of $f(\text{pH}) \propto \text{pH}^{-0.923}$ is only applicable in a certain pH range. The

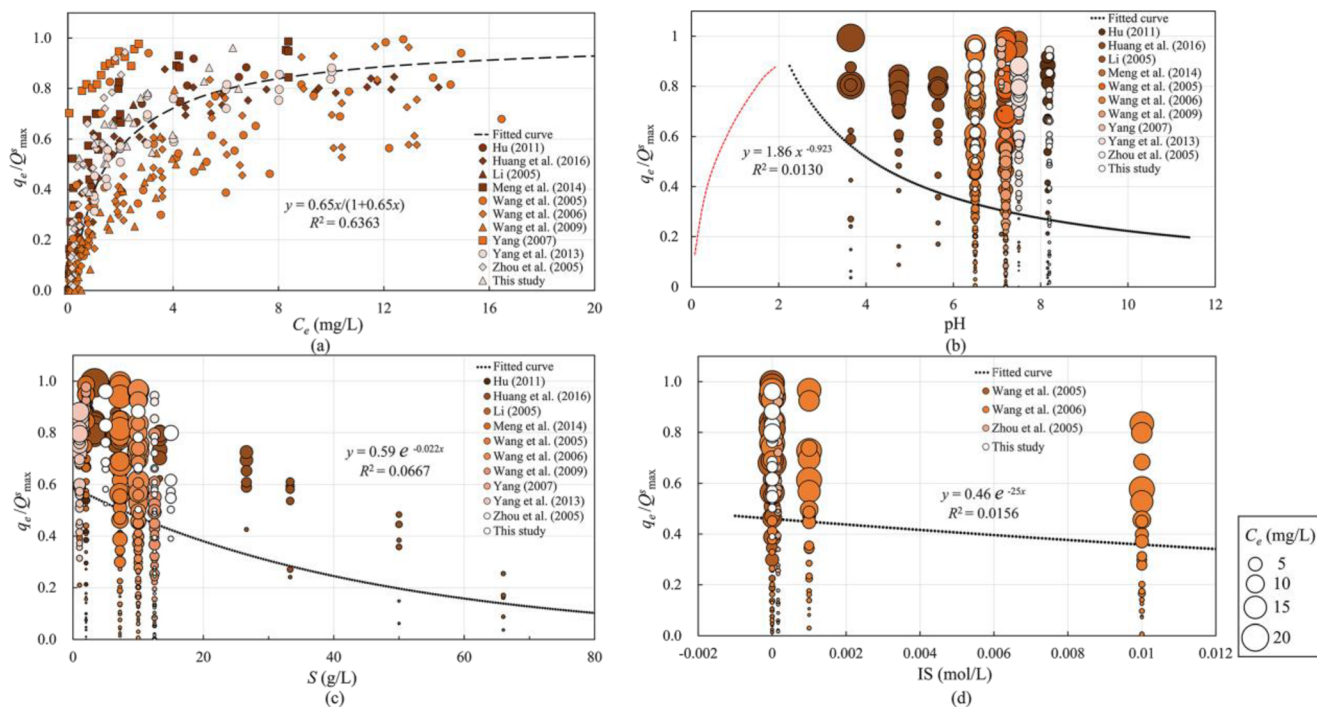


Fig. 4 The relation between q_e/Q_{max}^s and environmental factors. a C_e . b pH. c S . d IS . (Note: the sizes of the symbols in b–d represent the values of C_e)

Table 2 Individual factor and multivariable regression analysis of P adsorption by sediment. (Note: n is the number of data points, k_i and m_i are the fitting parameters, and R^2 is the correlation coefficient)

Individual factor				Multivariable regression					
C_e	pH	S	IS	C_e	pH	S	IS		
n	356	356	179	n	356				
k_i	0.650	-0.923	-0.022	-25	m_i	1.17	-0.32	-0.016	-13.8
R^2	0.6363	0.0130	0.0667	0.0156	R^2	0.7024			

correlation coefficient, R^2 , for each function is listed in Table 2. It is evident that amount of P adsorption is strongly correlated with C_e ($R^2 = 0.6363$), followed by S , IS , and pH.

The multivariable regression analysis was also conducted based on the same data set in Table A2 using 1stOpt software (see Eq. (9)) (where K is a proportional parameter and m_1 – m_4 are the parameters to be determined), and the results are listed in Table 2.

$$\frac{q_e}{Q_{\max}^s} = K \cdot \frac{m_1 C_e}{1 + m_1 C_e} \cdot \text{pH}^{m_2} \cdot e^{m_3 S} \cdot e^{m_4 \cdot IS} \quad (9)$$

As shown in Table 2, only 179 data points (among 356 data points) are used for the individual factor analysis of IS , as no information on IS was provided in the rest of the data points from the literature. Here, IS of the remaining 177 data points is simply assumed to be 0.0001 mol/L for the multivariable regression analysis (i.e., $n = 356$). Then, the function of multiple environmental factors is expressed as Eq. (10), and the corresponding R^2 is 0.7024.

$$\frac{q_e}{Q_{\max}^s} = 1.77 \cdot \frac{1.17 C_e}{1 + 1.17 C_e} \cdot \text{pH}^{-0.32} \cdot e^{-0.016 S} \cdot e^{-13.8 IS} \quad (10)$$

It is interesting that R^2 of the multivariable function only slightly increases from 0.6363 to 0.7024 compared with the individual function of C_e (i.e., Eq. (11)). Therefore, the inclu-

sion of pH, S , and IS may not significantly change the ability of the formula to describe P adsorption, and it is also acceptable to just apply Eq. (11) as a simplification.

$$\frac{q_e}{Q_{\max}^s} = \frac{0.65 C_e}{1 + 0.65 C_e} \quad (11)$$

Moreover, Fig. 5 shows the comparison between the measured and calculated amount of P adsorption, q_e/Q_{\max}^s , using Eqs. (10) and (11), where the dashed line indicates that the calculated values are equal to the measured values, i.e., $y = x$. Overall, the data points are close to the dashed line with a uniform distribution around the line in Fig. 5a, b, indicating that both equations can reasonably describe P adsorption, whereas Eq. (10) performs slightly better due to the incorporation of more environmental factors, which is closer to the actual conditions. Finally, P adsorption by sediment can be reliably predicted using Eqs. (4) and (10) or Eqs. (4) and (11), while simultaneously considering the effects of mineral composition and major environmental factors.

In this study, pure minerals were used to reveal the effects of mineral composition on P adsorption by sediment, and the effects of major environmental factors were also considered. It is worth noting that sediment from natural aqueous systems is generally coated with adsorbed substances, such as nitrogen (N), P, heavy metals, and microorganisms. Thus, P dynamics involve a great number of complex biotic and abiotic processes. Here, the influences of abiotic factors (i.e., mineral composition and environmental factors, including C_e , pH, IS , and S) were mainly considered while ignoring the impact of biological factors and other abiotic factors that also exert impacts on P adsorption under natural conditions. For example, Wang et al. (2007) found that the amount of P adsorption increased with increasing organic matter, which was one of the major factors controlling P adsorption by sediment. Chen (2017) concluded that the process of P adsorption by sediment was

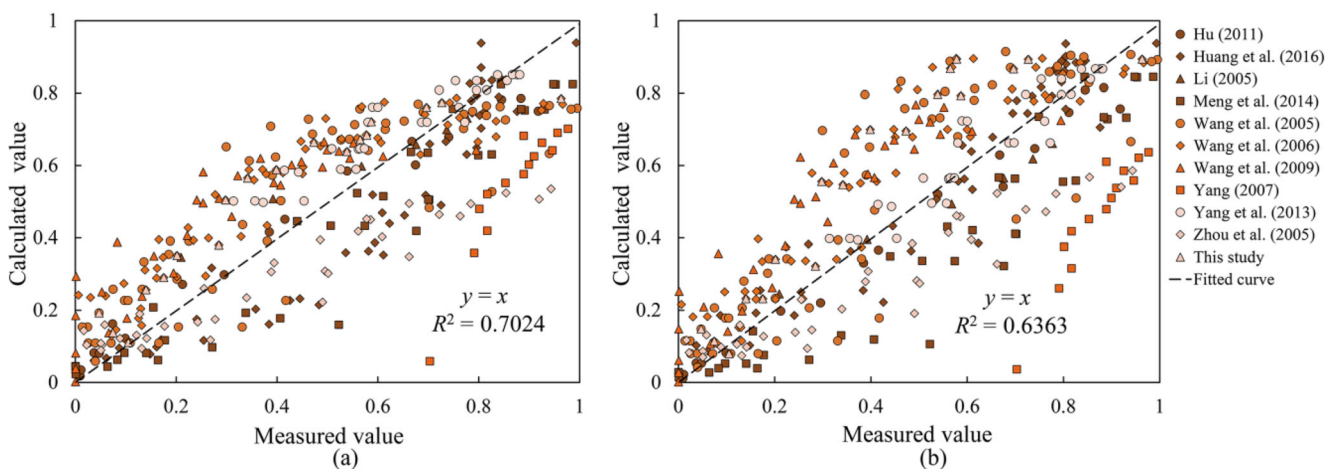


Fig. 5 Comparison between the measured and calculated amount of P adsorption, q_e/Q_{\max}^s , using **a** Eq. (10) and **b** Eq. (11)

affected by microorganisms due to the secretion of extracellular polymeric substances (EPS) through metabolism, which might enhance P adsorption. Moreover, the precipitation of iron oxide and P increases the amount of P adsorption by sediment, while the reduction of Fe^{3+} to Fe^{2+} results in P release when the redox potential decreases (Cooke et al. 2005). Therefore, it is necessary to further consider the effects of these biotic and abiotic factors on P adsorption by sediment in the future to provide references for practical engineering applications.

Conclusions

The P adsorption by sediment is affected by both internal factors (e.g., particle size and mineral composition) and external environmental factors (e.g., C_e , pH, IS , and S). In this study, P adsorption was studied from the perspective of mineral composition and a simple but general formula was proposed. The main conclusions are as follows:

- (1) Different minerals have different surface morphologies and lattice structures, leading to different adsorption properties. Although the contents of clay minerals are small in sediment, their P adsorption capacities are much larger than those of other minerals, which may greatly contribute to P adsorption.
- (2) Finer particles generally have a greater SSA and more potential surface-active sites, leading to a higher adsorption capacity. Furthermore, the mineral composition of sediment is also related to the particle size, i.e., a greater content of clay minerals can be observed in fine-grained sediment, which also affects P adsorption.
- (3) The amount of P adsorption is strongly correlated with C_e , followed by S , IS , and pH. Both the multivariable function (i.e., Eq. (10)) and the individual function of C_e (i.e., Eq. (11)) can reasonably predict the amount of P adsorption by sediment.

Overall, a formula that considers the external environmental factors from the perspective of pure minerals was proposed in this study, which can reliably predict P adsorption by sediment in different aqueous environments and can provide a foundation for the prediction of P dynamics.

Supplementary Information The online version contains supplementary material available at <https://doi.org/10.1007/s11356-020-12206-9>.

Acknowledgements The authors would like to thank the editors and anonymous reviewers for their valuable comments and suggestions.

Author contributions Xiaocui Li: Conceptualisation, writing of the original draft, methodology, investigation, formal analysis, visualization, and paper administration

Lei Huang: Writing of the original draft, formal analysis, conceptualisation, and paper administration

Hongwei Fang: Conceptualisation, writing, review, and editing, and paper administration

Minghong Chen, Zhenghui Cui, Zhiyu Sun, and Danny Reible: writing, review, and editing

Funding This research was funded by the 111 Project (No. B18031) and China Three Gorges Corporation (No. 201903145).

Data availability The experimental data are available from the corresponding author upon reasonable request.

Compliance with ethical standards

Ethical approval Not applicable.

Competing interests The authors declare that they have no competing interests.

References

- Aldegs Y, Elbarghouthi M, Elsheikh A, Walker G (2008) Effect of solution pH, ionic strength, and temperature on adsorption behavior of reactive dyes on activated carbon. *Dyes Pigments* 77:16–23
- An WC, Li XM (2009) Phosphate adsorption characteristics at the sediment–water interface and phosphorus fractions in Nansi Lake, China, and its main inflow rivers. *Environ Monit Assess* 148:173–184
- Chen YS (2017) Experiment on biofilm growth of cohesive sediment and effect on adsorption or desorption. Tsinghua University, Tsinghua (in Chinese)
- Chen ZH, Fang HW (2013) Analysis of the complex morphology of sediment particle surface based on electron microscope images. *Sci China Technol Sci* 56:280–285
- Cooke GD, Welch EB, Peterson S, Nichols S (2005) Restoration and management of lakes and reservoirs. CRC Press, Boca Raton
- Cui ZH, Fang HW, Huang L, Ni K, Reible D (2017) Effect of surface heterogeneity on phosphorus adsorption onto mineral particles: experiments and modeling. *J Soils Sediments* 17:2887–2898
- Davis JA, Coston JA, Kent DB, Fuller CC (1998) Application of the surface complexation concept to complex mineral assemblages. *Environ Sci Technol* 32:2820–2828
- Dickens AF, Baldock JA, Smernik RJ, Wakeham SG, Arnarson TS, Gélinas Y, Hedges JI (2006) Solid-state ^{13}C NMR analysis of size and density fractions of marine sediments: insight into organic carbon sources and preservation mechanisms. *Geochim Cosmochim Acta* 70:666–686
- Edzward JK, Toensing DC, Leung CY (1976) Phosphate adsorption reactions with clay minerals. *Environ Sci Technol* 10:485–490
- Fang HW, Chen MH, Chen ZH (2008) Surface pore tension and adsorption characteristics of polluted sediment. *Sci China, Ser G* 51:1022–1028
- Fang HW, Chen MH, Chen ZH (2013) Effects of sediment particle morphology on adsorption of phosphorus elements. *Int J Sediment Res: English version* 28:246–253
- Fang HW, Chen MH, Chen ZH, Zhao HM, He GJ (2014) Simulation of sediment particle surface morphology and element distribution by the concept of mathematical sand. *JHydro-Environ Res* 8:186–193
- Fang HW, Cui ZH, He GJ, Huang L, Chen MH (2017) Phosphorus adsorption onto clay minerals and iron oxide with consideration of heterogeneous particle morphology. *Sci Total Environ* 605:357–367

- Foo KY, Hameed BH (2010) Insights into the modeling of adsorption isotherm systems. *Chem Eng J* 156:2–10
- Furumai H, Kondo T, Ohgaki S (1989) Phosphorus exchange kinetics and exchangeable phosphorus forms in sediments. *Water Res* 23: 685–691
- Gao L, Zhang LH, Shao HB (2014) Phosphorus bioavailability and release potential risk of the sediments in the coastal wetland: a case study of Rongcheng Swan Lake, Shandong, China. *CLEAN-Soil Air Water* 42:963–972
- Gérard F (2016) Clay minerals, iron/aluminum oxides, and their contribution to phosphate sorption in soils — a myth revisited. *Geoderma* 262:213–226
- Hayes KF, Redden G, Ela W, Leckie JO (1991) Surface complexation models—an evaluation of model parameter-estimation using FITEQL and oxide mineral titration data. *J Colloid Interface Sci* 142:448–469
- He GJ, Fang HW, Bai S, Liu XB, Chen MH, Bai J (2011) Application of a three-dimensional eutrophication model for the Beijing Guanting Reservoir, China. *Ecol Model* 222:1491–1501
- Hei PS, Zhang YY, Shang YZ, Lei XH, Quan J, Zhang M (2017) An approach to minimizing the uncertainty caused by sediment washing pretreatment in phosphorus adsorption experiments. *Ecol Eng* 107: 244–251
- Huang LD, Fu LL, Jin CW, Gielen G, Lin XY, Wang HL, Zhang YS (2011) Effect of temperature on phosphorus sorption to sediments from shallow eutrophic lakes. *Ecol Eng* 37:1515–1522
- Huang L, Fang HW, Reible D (2015a) Mathematical model for interactions and transport of phosphorus and sediment in the Three Gorges Reservoir. *Water Res* 85:393–403
- Huang L, Fang HW, Fazeli M, Chen YS, Chen DY, He GJ (2015b) Mobility of phosphorus induced by sediment resuspension in the Three Gorges Reservoir by flume experiment. *Chemosphere* 134: 374–379
- Huang L, Fang HW, He GJ, Chen MH (2016) Phosphorus adsorption on natural sediments with different pH incorporating surface morphology characterization. *Environ Sci Pollut Res* 23:18883–18891
- Huang L, Fang HW, Xu XY, He GJ, Zhang XS, Reible D (2017) Stochastic modeling of phosphorus transport in the Three Gorges Reservoir by incorporating variability associated with the phosphorus partition coefficient. *Sci Total Environ* 592:649–661
- Hu K (2011) Physical and chemical properties of sediment in the Yellow River and its adsorption behavior for phosphorus. Beijing Forestry University, Beijing (in Chinese)
- Jarvie HP, Jurgens MD, Williams RJ, Neal C, Davies JLL, Barrett C, White J (2005) Role of river bed sediments as sources and sinks of phosphorus across two major eutrophic UK river basins: the Hampshire Avon and Herefordshire Wye. *J Hydrol* 304:51–74
- Jin XC, Wang SR, Pang Y, Zhao HC, Zhou XN (2005) The adsorption of phosphate on different trophic lake sediments. *Colloids Surf A-Physicochem Eng Aspects* 254:241–248
- Kafkafi U, Baryosef BY, Rosenberg R, Sposito G (1988) Phosphorus adsorption by kaolinite and montmorillonite: II Organic anion competition. *Soil Sci Soc Am J* 52:1585–1589
- Ku WC, Digiano FA, Feng TH (1978) Factors affecting phosphate adsorption equilibria in lake-sediments. *Water Res* 12:1069–1074
- Langmuir I (1916) The constitution and fundamental properties of solids and liquids part I solids. *J Am Chem Soc* 38:2221–2295
- Langmuir I (1917) The constitution and fundamental properties of solids and liquids II Liquids. *J Am Chem Soc* 39:1848–1906
- Langmuir I (1918) The adsorption of gases on plane surfaces of glass, mica and platinum. *J Am Chem Soc* 40:1361–1403
- Liu ZF, Lee C (2007) The role of organic matter in the sorption capacity of marine sediments. *Mar Chem* 105:240–257
- Li M, Ni J, Wang G, Wei H (2005) Study on the influence of environmental factors on phosphate adsorption by sediments in the Yangtze River Estuary. *J Basic Sci Eng* 19–25
- Li C (2005) Study on the effect of sediment on eutrophication in Chongqing section of Three Gorges Reservoir area. Chongqing University, Chongqing (in Chinese)
- Li G, Xiao S, Wang Y, Liu L, Niu F (2012) Grain size distribution and mineral composition of sediments in the main stream of the Three Gorges Reservoir. *J Three Gorges Univ (Natural Science Edition)* 34:9–13
- Li XC, Huang L, Fang HW, He GJ, Reible D, Wang CH (2019) Immobilization of phosphorus in sediments by nano zero-valent iron (nZVI) from the view of mineral composition. *Sci Total Environ* 694:133695
- Lopez P, Lluç X, Vidal M, Morgui JA (1996) Adsorption of phosphorus on sediments of the Balearic Islands (Spain) related to their composition. *Estuar Coast Shelf Sci* 42:185–196
- Malek A, Farooq S (1996) Comparison of isotherm models for hydrocarbon adsorption on activated carbon. *AIChE J* 42:3191–3201
- Meng J, Yao QZ, Yu ZG (2014) Particulate phosphorus speciation and phosphate adsorption characteristics associated with sediment grain size. *Ecol Eng* 70:140–145
- Ministry of Environment Protection of China (MEP) (2001) Water quality - determination of total phosphorus ammonium molybdate-spectrophotometric method. Natl. Stand. of China, China Standard Press, Beijing (in Chinese)
- Mortula M, Gibbons M, Gagnon GA (2007) Phosphorus adsorption by naturally-occurring materials and industrial by-products. *J Environ Eng Sci* 6:157–164
- Pagnanelli F, Esposito A, Toro L, Veglio F (2003) Metal speciation and pH effect on Pb, Cu, Zn and Cd biosorption onto *Sphaerotilus natans*: Langmuir-type empirical model. *Water Res* 37:627–633
- Palleyi S, Banoo S, Kar RN, Panda CR (2015) Textural and geochemical characteristics of off shore sediment of North Bay of Bengal: a statistical approach for marine metal pollution. *Int J Sediment Res* 30(3):208–222
- Prarat P, Ngamcharussrivichai C, Khaodhiar S, Punyapalaku P (2011) Adsorption characteristics of haloacetonitriles on functionalized silica-based porous materials in aqueous solution. *J Hazard Mater* 192:1210–1218
- Schaller MS, Landry CJ, Koretsky CM, Lund TJ, Soumya D (2008) Surface complexation modeling of Cu(II) adsorption on mixtures of hydrous ferric oxide and kaolinite. *Geochim Cosmochim Acta* 9:9–9
- Selig U (2003) Particle size-related phosphate binding and P-release at the sediment-water interface in a shallow German lake. *Hydrobiologia* 492(1–3):107–118
- Shao XX, Liang XQ, Wu M, Gu BH, Li WH, Sheng XC, Wang SX (2014) Influences of sediment properties and macrophytes on phosphorus speciation in the intertidal marsh. *Environ Sci Pollut Res* 21:10432–10441
- Shi ZL, Wang YY, Wen AB, Yan DC, Chen JC (2018) Temporal-spatial variations of sediment-associated nutrients and contaminants in the Ruxi tributary of the Three Gorges Reservoir, China. *J Mt Sci* 15: 319–326
- Stone M, Mudroch A (1989) The effect of particle size, chemistry and mineralogy of river sediments on phosphate adsorption. *Environ Technol Lett* 10:501–510
- Sundareshwar PV, Morris JT (1999) Phosphorus sorption characteristics of intertidal marsh sediments along an estuarine salinity gradient. *Limnol Oceanogr* 44:1693–1701
- Tang HX, Qian Y, Wen XH (2000) Characteristics and control principles of water particles and refractory organics. Volume II. Refractory organics. Environmental Science Press, Beijing: China (in Chinese)
- Tang XQ, Wu M, Dai XC, Chai PH (2014) Phosphorus storage dynamics and adsorption characteristics for sediment from a drinking water source reservoir and its relation with sediment compositions. *Ecol Eng* 64:276–284

- Uddin MK (2017) A review on the adsorption of heavy metals by clay minerals, with special focus on the past decade. *Chem Eng J* 308: 438–462
- Ushiki I, Ota M, Sato Y, Inomata H (2014) Prediction of VOCs adsorption equilibria on activated carbon in supercritical carbon dioxide over a wide range of temperature and pressure by using pure component adsorption data: combined approach of the Dubinin-Astakhov equation and the non-ideal adsorbed solution theory (NIAST). *Fluid Phase Equilib* 375:293–305
- Venema P, Hiemstra T, Weidler PG, van Riemsdijk WH (1998) Intrinsic proton affinity of reactive surface groups of metal (hydr)oxides: application to iron (hydr)oxides. *J Colloid Interface Sci* 198:282–295
- Wang SG, Jin XC, Pang Y, Zhao HC, Zhou XN, Wu FC (2005) Phosphorus fractions and phosphate sorption characteristics in relation to the sediment compositions of shallow lakes in the middle and lower reaches of Yangtze River region, China. *J Colloid Interface Sci* 289:339–346
- Wang SR, Jin XC, Bu QY, Zhou XN, Wu FC (2006) Effects of particle size, organic matter and ionic strength on the phosphate sorption in different trophic lake sediments. *J Hazard Mater* 128:95–105
- Wang SR, Jin XC, Zhao HC, Zhou XN, Wu FC (2007) Effect of organic matter on the sorption of dissolved organic and inorganic phosphorus in lake sediments. *Colloids Surf A Physicochem Eng Asp* 297: 154–162
- Wang Y, Shen ZY, Niu JF, Liu RM (2009) Adsorption of phosphorus on sediments from the Three-Gorges Reservoir (China) and the relation with sediment compositions. *J Hazard Mater* 162:92–98
- Wang L, Zhao XH, Zhang JM, Xiong ZH (2017) Selective adsorption of Pb (II) over the zinc-based MOFs in aqueous solution-kinetics, isotherms, and the ion exchange mechanism. *Environ Sci Pollut Res* 24:14198–14206
- Wakeham SG, Canuel EA, Lerberg EJ, Mason P, Sampere TP, Bianchi TS (2009) Partitioning of organic matter in continental margin sediments among density fractions. *Mar Chem* 115(3–4):211–225
- White GN, Zelazny LW (1988) Analysis and implications of the edge structure of dioctahedral phyllosilicates. *Anal Clays Clay Miner* 36: 141–146
- Wieland E, Stumm W (1992) Dissolution kinetics of kaolinite in acidic aqueous-solutions at 25-degrees-C. *Geochim Cosmochim Acta* 56: 3339–3355
- Xu H, Paerl HW, Qin BQ, Zhu GW, Gao G (2010) Nitrogen and phosphorus inputs control phytoplankton growth in eutrophic Lake Taihu, China. *Limnol Oceanogr* 55:420–432
- Yang SY, Jung HS, Choi MS, Li CX (2002) The rare earth element compositions of the Changjiang (Yangtze) and Huanghe (Yellow) river sediments. *Earth Planet Sci Lett* 201(PII S0012-821X(02)00715-X2):407–419
- Yang C (2007) Study on the influencing factors of phosphate adsorption and desorption of suspended sediment in the Three Gorges Reservoir area. Chongqing University (in Chinese)
- Yang X, Zhu XL, Cheng HK, Li KJ, Lu Q, Liang DF (2013) Characteristics of phosphorus adsorption by sediment mineral matrices with different particle sizes. *Water Sci Eng* 6:262–271
- Zhang TX, Wang XR, Jin XC (2007) Variations of alkaline phosphatase activity and P fractions in sediments of a shallow Chinese eutrophic lake (Lake Taihu). *Environ Pollut* 150:288–294
- Zhang Y (2017) Phosphorus adsorption and desorption characteristics of sediment in the Three Gorges Reservoir area. Central University for Nationalities (in Chinese)
- Zhao HM, Fang HW, Cheng MH (2011) Floc architecture of bioflocculation sediment by ESEM and CLSM. *Scanning* 33:437–445
- Zhao Y, Yang SK, Li HH, Wang D (2015) Adsorption behaviors of acetaminophen onto sediment in the Weihe River, Shaanxi, China. *Int J Sediment Res* 30:263–271
- Zhou AM, Tang HX, Wang DS (2005) Phosphorus adsorption on natural sediments: modeling and effects of pH and sediment composition. *Water Res* 39:1245–1254

Publisher's note Springer Nature remains neutral with regard to jurisdictional claims in published maps and institutional affiliations.